drogen atoms were placed at their geometrically calculated positions (C-H = 1.00 Å) and refined "riding" on the corresponding carbon atoms. The final cycles of refinement were carried out on the basis of 463 (1), 478 (2), and 418 (3) variables; after the last cycles, no parameters shifted by more than 0.86 (1), 0.50 (2), and 0.81 (3) esd. The biggest remaining peaks in the final difference maps were equivalent to about 0.52 (1), 0.97 (2), and 0.81 (3) e/Å^3. In the final cycles of refinement a weighting scheme, $w = K[\sigma^2(F_o) + gF_o^2]^{-1}$, was used; at convergence the K values were 0.335 (1), 0.544 (2), and 0.366 (3), and the g values 0.0013 (1), 0.0033 (2), 0.0018 (3). The analytical scattering factors, corrected for the real and imaginary parts of anomalous dispersions, were taken from ref 11. The final atomic coordinates for the non hydrogen atoms are given in Tables V (anion 1), VI (cation 1), VII (2), and VIII (3). The atomic coordinates of the hydrogen atoms are given in Tables SI (1), SII (2), SIII (3); the thermal parameters in Tables SIV and SV (1), SVI (2), and SVII (3) (see supplementary material paragraph).

(11) *International Tables for X-Ray Crystallography*; Kynoch Press: Birmingham, England, 1974; Vol. IV.

Acknowledgments. We are grateful for financial support of this work by the Fonds National Suisse de la Recherche Scientifique and the Stiftung Volkswagenwerk. A generous loan of ruthenium trichloride hydrate by the Johnson Matthey Technology Centre is gratefully acknowledged. We also thank Prof. Ulrich Koelle, Aachen University of Technology, for helpful discussions.

Registry No. [$(PPh_3)_2N$][1], 126294-88-0; Na[1], 126294-91-5; **2**, 126294-89-1; **3**, 126294-90-4; $Na[HRu_3(CO)_{11}]$, 71936-71-5; $Ru_3(CO)_{12}$, 15243-33-1; $(PPh_3)_3RhCl$, 14694-95-2; $(PPh_3)_2Ir(CO)Cl$, 14871-41-1; Ru, 7440-18-8; Ir, 7439-88-5; Rh, 7440-16-6.

Supplementary Material Available: Tables SI, SII, and SIII (atomic coordinates and isotropic thermal parameters for the hydrogen atoms) and Tables SIV, SV, SVI and SVII (thermal parameters for the non-hydrogen atoms) (113 pages); tables of observed and calculated structure factors (108 pages). Ordering information is given on any current masthead page.

Reactivity Patterns for Multisite-Bound Acetylides. Nucleophilic Attack at the α-Carbon in μ_2-η^2-Acetylides. Bridging 2-Amino-1-metallaphenethylidene Complexes via Addition of Primary Amines to $M_2(CO)_6(\mu_2$-η^2-C≡CPh)(μ-PPh_2) (M = Fe, Ru, Os)

Andrew A. Cherkas, Leslie H. Randall, Nicholas J. Taylor, Graham N. Mott, John E. Yule, Jean Luc Guinamant, and Arthur J. Carty*

Guelph-Waterloo Centre for Graduate Work in Chemistry, Waterloo Campus, Department of Chemistry, University of Waterloo, Waterloo, Ontario, Canada N2L 3G1

Received September 12, 1989

The binuclear σ-π-acetylides $M_2(CO)_6(\mu_2$-η^2-C≡CPh)(μ-PPh_2) (**1a**, M = Fe; **1b**, M = Ru; **1c**, M = Os) react with cyclohexylamine to form the two-carbon-bridged iminium complexes $M_2(CO)_6[\mu_2$-C{NHR}CH-(Ph)](μ-PPh_2) (**3a-c**, R = c-C_6H_{11}) in all three cases by attack at the α-carbon of the acetylide of 1 and proton transfer across the acetylide triple bond. The new ligands in **3a-c** are 2-(cyclohexylamino)-1-metallaphenethylidene derivatives with a carbene-like carbon atom coordinated to one metal and an sp^3 carbon atom, derived from C_β of the acetylide attached to the second metal. Analogous complexes M_2-$(CO)_6[\mu_2$-C{NH(*i*-Pr)}CH(Ph)](μ-PPh_2) (M = Ru, **5b**; M = Os, **5c**) have been characterized from the reactions of **1b** and **1c** with isopropylamine. Complex **1a** only also forms the product of β-acetylide addition $M_2(CO)_6[\mu_2$-CHC(NRH)Ph](μ-PPh_2). The entire triad of two-carbon-bridged products from **1a-c** with cyclohexylamine, $M_2(CO)_6[\mu_2$-C{NH(Cy)}CH(Ph)](μ-PPh_2) (**3a-c**), have been characterized by IR and ^{1}H, ^{13}C{^{1}H}, and ^{31}P{^{1}H} NMR spectroscopy and by single-crystal X-ray diffraction. Crystals of **3b,c** are monoclinic space group $P2_1/c$ with the following unit cell dimensions: **3b**, a = 10.076 (3), b = 17.290 (4), c = 20.807 (4) Å, β = 102.18 (2)°, Z = 4; **3c**, a = 10.164 (2), b = 17.126 (5), c = 20.691 (5) Å, β = 99.44 (2)°, Z = 4. The two structures were solved by the heavy-atom method and refined to the following R and R_w values: **3b**, R = 0.030, R_w = 0.035 on 4372 observed diffractometer data; **3c**, R = 0.035, R_w = 0.038 on 4051 observed data. Comparison with the structure of **3a** determined earlier shows that all three molecules are isostructural, with M-M bond lengths of 2.628 (1) Å for **3a**, 2.7896 (4) Å for **3b**, and 2.8197 (5) Å for **3c**. Changes in the metal-hydrocarbyl interactions down the triad are discussed.

Introduction

As a C_2 hydrocarbyl with the highest degree of unsaturation and unsurpassed versatility as a bridging ligand, the alkynyl or acetylide ligand continues to attract attention.[1] Mononuclear η^1-acetylides have been shown to react with electrophiles at the β-carbon atom to form vinylidenes that can, in turn, be converted to other hydrocarbyls.[2] Theoretical calculations by Kostic and Fenske[3] suggest that this sequence of reactions has components of orbital and charge control. The reactivity of μ_3-η^2-acetylides toward nucleophiles, which has been studied extensively by Deeming and co-workers[4] and ourselves,[5] is dominated by attack at C_α although reaction at C_β has been observed.[4a] Semiempirical CNDO calculations by Grannozzi et al.[6] have indicated that the regiospecificity of these reactions is charge controlled.

0276-7333/90/2309-1677$02.50/0

Edge-bridging μ_2-η^2-acetylides also have a rich chemistry not only as sources of μ-vinylidenes[7a] and other hydrocarbyls[7b-i,8,9] but also for mixed-metal cluster construction.[10] Extensive work has been carried out in this laboratory on the reactivity of $Fe_2(CO)_6(\mu_2$-η^2-C≡CR)(μ-PPh_2), including **1a**, toward nitrogen,[7c-f] phosphorus,[7a,b] and carbon[7g-i] nucleophiles. Seyferth's group has recently reported closely similar reactivity for the thiolato-bridged acetylides $Fe_2(CO)_6(\mu_2$-η^2-C≡CR′)(μ-SR).[9] In these systems the nucleophile can add at the β-carbon of the acetylide to form a one carbon bridged product, or at the acetylide α-carbon atom to form a two carbon bridge (Scheme I). With primary and secondary amines, a hydrogen atom from the amine is also added across the triple bond (Scheme II) to form either a zwitterionic μ-alkylidene (β-addition) or a two-carbon iminium zwitterion (α-addition).

We have now characterized the complete triad of μ_2-η^2-acetylide complexes $M_2(CO)_6(\mu_2$-η^2-C≡CR)(μ-PPh_2) (**1**, M = Fe (**a**), M = Ru (**b**), M = Os (**c**); R = Ph, *t*-Bu, *i*-Pr][11] and recently described the triad of μ-alkylidene products

Scheme I[a]

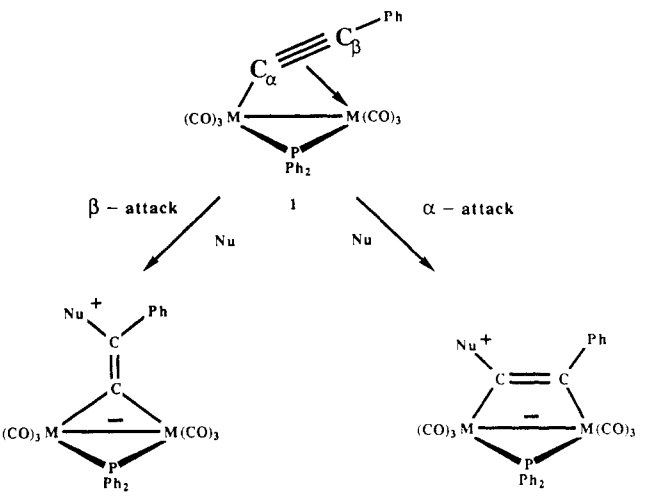

[a] Nu = nucleophile.

Scheme II

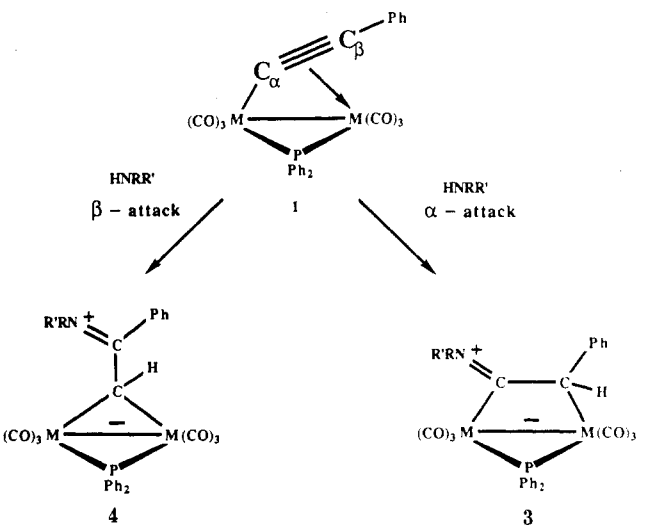

$M_2(CO)_6[\mu$-CHC(NEt_2)Ph](μ-PPh_2) (M = Fe **2a**; M = Ru, **2b**; M = Os, **2c**) from the addition of diethylamine to **1** (R = Ph).[12]

As part of our comparative reactivity studies for the triad **1**, we have completed initial investigations of the two-carbon-bridged product $Fe_2(CO)_6[\mu$-C{NH(Cy)}CH(Ph)](μ-PPh_2) (**3a**)[7e] and extended the work to the ruthenium and osmium complexes $M_2(CO)_6[\mu$-C{CyNH}CH(Ph)](μ-PPh_2) (M = Ru, **3b**; M = Os, **3c**; Cy = cyclohexyl). Spectroscopic (IR, ^1H, $^{13}C\{^1H\}$, $^{31}P\{^1H\}$ NMR) and single-crystal X-ray analyses (**3b**, **3c**) are reported herein. A subsequent paper detailing EHMO modeling of orbital and charge factors controlling these reactions will follow.

Experimental Section

General Procedures. Standard Schlenk line techniques were used, and manipulations were carried out under a nitrogen atmosphere. Solvents were dried (heptane and toluene over $LiAlH_4$), deoxygenated, and distilled before use. Deuteriochloroform for NMR studies was stored over Linde molecular sieves. Cyclohexylamine and isopropylamine were purchased from Aldrich Chemical Co. and used as received. Infrared spectra were recorded on a Perkin-Elmer 180 spectrometer as solutions in 0.5-mm matched sodium chloride cells or as Nujol mulls on a Perkin-Elmer 983 spectrometer between sodium chloride plates. NMR spectra

(1) For reviews on acetylide chemistry see: (a) Sappa, E.; Tiripicchio, A.; Braunstein, P. *Chem. Rev.* **1983**, *83*, 202. (b) Nast, R. *Coord. Chem. Rev.* **1982**, *47*, 89. (c) Carty, A. J. *Pure Appl. Chem.* **1982**, *54*, 113. (d) Raithby, P. R.; Rosales, M. J. *Adv. Inorg. Radiochem.* **1986**, *29*, 169. For some recent work see: (e) Deeming, A. J.; Felix, M. S. B.; Bates, P. A.; Hursthouse, M. B. *J. Chem. Soc., Chem. Commun.* **1987**, 461. (f) Mercer, R. J.; Green, M.; Orpen, A. G. *J. Chem. Soc., Chem. Comun.* **1986**, 567. (g) Alcock, N. W.; Kemp, T. J.; Pringle, P. G.; Bergamini, P.; Traverso, O. *J. Chem. Soc., Dalton Trans.* **1987**, 1659. (h) Suades, J.; Dahan, F.; Mathieu, R. *Organometallics* **1988**, *7*, 16. (i) Nucciarone, D.; MacLaughlin, S. A.; Taylor, N. J.; Carty, A. J. *Organometallics* **1988**, *7*, 106. (j) Nucciarone, D.; Taylor, N. J.; Carty, A. J.; Tiripicchio, A.; Camellini, M. T.; Sappa, E. *Organometallics* **1988**, *7*, 118. (k) Nucciarone, D.; Taylor, N. J.; Carty, A. J. *Organometallics* **1988**, *7*, 127. (l) Bruce, M. I.; Liddell, M. J.; Snow, M. R.; Tiekink, E. R. *Organometallics* **1988**, *7*, 343. (m) Sappa, E. *J. Organomet. Chem.* **1987**, *323*, 83. (n) Blau, R. J.; Chisholm, M. H.; Folting, K.; Wang, R. J. *J. Am. Chem. Soc.* **1987**, *109*, 4552. (o) Koridze, A. A.; Kizas, Q. A.; Petrovskii, P. V.; Kolobova, N. E.; Struchkov, Y. T.; Yanovsky, A. I. *J. Organomet. Chem.* **1988**, *338*, 81. (p) Marder, T. B.; Zargarian, D.; Calabrese, J. C.; Herskovitz, T. H.; Milstein, D. *J. Chem. Soc., Chem. Commun.* **1987**, 1484. (q) Carriedo, G. A.; Miguel, D.; Riera, V.; Solons, X. *J. Chem. Soc., Dalton Trans.* **1987**, 2867. (r) Fontaine, X. L. R.; Higgins, S. J.; Langrick, C. R.; Shaw, B. L. *J. Chem. Soc., Dalton Trans.* **1987**, 777. (s) Ewing, P.; Farrugia, L. J. *Organometallics* **1989**, *8*, 1246.

(2) (a) Bruce, M. I.; Swincer, A. G. *Aust. J. Chem.* **1980**, *33*, 1471. (b) Davidson, A.; Selegue, J. P. *J. Am. Chem. Soc.* **1980**, *102*, 2455. (c) Davidson, A.; Selegue, J. P.; *J. Am. Chem. Soc.* **1978**, *100*, 7763.

(3) Kostic, N. M.; Fenske, R. F. *Organometallics* **1982**, *1*, 974.

(4) (a) Boyar, E.; Deeming, A. J.; Kabir, S. E. *J. Chem. Soc., Chem. Commun.* **1986**, 577. (b) Aime, S.; Deeming, A. J. *J. Chem. Soc., Dalton Trans.* **1983**, 1807. (c) Henrick, K.; McPartlin, M.; Deeming, A. J.; Hasso, S.; Manning, P. J. *J. Chem. Soc., Dalton Trans.* **1982**, 899. (d) Deeming, A. J.; Hasso, S. *J. Organomet. Chem.* **1976**, *112*, C39.

(5) MacLaughlin, S. A.; Johnson, J. P.; Taylor, N. J.; Carty, A. J.; Sappa, E. *Organometallics* **1983**, *2*, 352.

(6) Granozzi, G.; Tondello, E.; Bertoncello, R.; Aime, S.; Osella, D. *Inorg. Chem.* **1983**, *22*, 744.

(7) (a) Carty, A. J.; Mott, G. N.; Taylor, N. J.; Ferguson, G.; Khan, M. A.; Roberts, P. J.; *J. Organomet. Chem.* **1978**, *149*, 345. (b) Wong, Y. S.; Paik, H. N.; Chieh, P. C.; Carty, A. J. *J. Chem. Soc., Chem. Commun.* **1975**, 309. (c) Carty, A. J.; Taylor, N. J.; Paik, H. N.; Smith, W.; Yule, J. G. *J. Chem. Soc., Chem. Commun.* **1976**, 41. (d) Carty, A. J.; Mott, G. N.; Taylor, N. J. *J. Organomet. Chem.* **1979**, *182*, C69. (e) Carty, A. J.; Mott, G. N.; Taylor, N. J.; Yule, J. E. *J. Am. Chem. Soc.* **1978**, *100*, 3051. (f) Mott, G. N.; Carty, A. J. *Inorg. Chem.* **1983**, *22*, 2726. (g) Smith, W. F.; Taylor, N. J.; Carty, A. J. *J. Chem. Soc., Chem. Commun.* **1976**, 896. (h) Carty, A. J.; Taylor, N. J.; Smith, W. F.; Lappert, M. F.; Pye, P. L. *J. Chem. Soc., Chem. Commun.* **1978**, 1017. (i) Carty, A. J.; Mott, G. N.; Taylor, N. J. *J. Organomet. Chem.* **1981**, *212*, C54.

(8) Nubel, P. O.; Brown, T. L. *Organometallics* **1984**, *3*, 29.

(9) Seyferth, D.; Hoke, J. B.; Wheeler, D. R. *J. Organomet. Chem.* **1988**, *341*, 421.

(10) (a) Koridze, A. A.; Kizas, O. A.; Kolobova, N. E.; Vinogradova, V. N.; Ustynyuk, N. A.; Petrovskii, P. V.; Yanovsky, A. I.; Struchkov, Y. T. *J. Chem. Soc., Chem. Commun.* **1984**, 1158. (b) Weatherell, C.; Taylor, N. J.; Carty, A. J.; Sappa, E.; Tiripicchio, A. *J. Organomet. Chem.* **1985**, *291*, C9. (c) Seyferth, D.; Hoke, J. B.; Rheingold, A. L.; Cowie, M.; Hunter, A. D. *Organometallics* **1988**, *7*, 2163.

(11) Cherkas, A. A.; Randall, L. H.; MacLaughlin, S. A.; Mott, G. N.; Taylor, N. J.; Carty, A. J. *Organometallics* **1988**, *7*, 969.

(12) Cherkas, A. A.; Mott, G. N.; Granby, R.; MacLaughlin, S. A.; Yule, J. E.; Taylor, N. J.; Carty, A. J. *Organometallics* **1988**, *7*, 1115.

were measured on a Bruker AM-250 instrument (^{1}H, 250 MHz; ^{31}P{^{1}H}, 101.3 MHz; ^{13}C{^{1}H}, 62.8 MHz), and shifts referenced internally to Me_4Si (^{1}H, ^{13}C) or externally to 85% H_3PO_4 (^{31}P). ^{13}C NMR assignments were facilitated by use of the JMODX, spin echo pulse sequence.[13] Microanalyses were carried out by Guelph Chemical Laboratories, Guelph, Ontario, Canada.

Syntheses. Complexes **1a–c**, R = Ph, were prepared as described elsewhere,[11] as were complexes **3a** and **4**.[7e] The spectroscopic data for **3a** and **4** are updated here, and the new ^{13}C{^{1}H} spectral data added.

$Fe_2(CO)_6[\mu$-C{NH(Cy)}CH(Ph)](μ-PPh$_2$) (3a). This complex was prepared as previously described.[7e] IR (C_6H_{12}) ν(CO) 2055 s, 2012 vs, 1984 s, 1965 s, 1945 m cm^{-1}; (Nujol mull) ν(N–H) 3280 w; ν(C=N) 1521 m cm^{-1}. ^{1}H NMR (250 MHz, $CDCl_3$) δ 7.67 (m, Ph-*H*), 7.40–6.88 (m, Ph-*H*), 6.56 (d, N*H*, $^3J_{H-H}$ = 7.5 Hz), 5.38 (m, NC*H*), 2.68 (d, C$_\beta$H, $^3J_{P-H}$ = 13.0 Hz), 2.16–0.77 (m, Cy-CH_2). ^{31}P{^{1}H} (24.3 MHz, C_6D_6) δ 183.5 (s). ^{13}C{^{1}H} NMR (62.8 MHz, $CDCl_3$) δ 234.3 (d, C$_\alpha$, $^2J_{P-C}$ = 11.2 Hz), 215.5 (d, CO$_2$, $^2J_{P-C}$ = 31.5 Hz), 213.9 (s, CO$_1$), 212.8 (br s, CO$_{4,5,6}$), 211.3 (d, CO$_3$, $^2J_{P-C}$ = 16.4 Hz), 144.0 (d, C$_i$″, $^3J_{P-C}$ = 8.2 Hz), 140.6 (d, C$_i$, $^1J_{P-C}$ = 39.3 Hz), 138.1 (d, C$_i$″, $^1J_{P-C}$ = 24.2 Hz), 134.1 (d, C$_o$, $^2J_{P-C}$ = 7.5 Hz), 133.8 (d, C$_o$′, $^2J_{P-C}$ = 7.7 Hz), 129.6 (s, C$_p$), 129.5 (s, C$_p$′), 129.2 (s, C$_o$″), 128.5 (d, C$_m$, $^3J_{P-C}$ = 10.3 Hz), 128.3 (d, C$_m$′, $^3J_{P-C}$ = 10.2 Hz), 126.6 (s, C$_m$″, 125.3 (s, C*p*″), 58.9 (s, Cy-*C*N), 44.9 (d, C$_\beta$, $^2J_{P-C}$ = 3.9 Hz), 33.7 (s, Cy-*C*H$_2$), 31.5 (s, Cy-*C*H$_2$′), 25.1 (s, Cy-*C*H$_2$″), 25.0 (s, Cy-CH$_2$‴), 22.8 (s, CyCH$_2$⁗).

$Fe_2(CO)_6[\mu$-CHC{N(Cy)H}(Ph)](μ-PPh$_2$) (4). This β-adduct was prepared as described earlier.[7e] IR (C_6H_{12}) ν(CO) 2033 m, 1999 vs, 1956 s br, 1913 w cm^{-1}; (Nujol mull) ν(N–H) 3280 w cm^{-1}, ν(C=N), 1547 m cm^{-1}. ^{1}H NMR (250 MHz, $CDCl_3$) δ 7.85 (m, Ph-*H*), 7.56–7.12 (m, Ph-*H*); 6.93 (d, NH, $^3J_{H-H}$ = 7.1 Hz, 3.24 (m, NC*H*), 1.58 (d, C$_\alpha$H, $^3J_{P-H}$ = 34.4 Hz), 1.78–0.78 (m, Cy-CH_2). ^{31}P{^{1}H} (24.3 MHz, C_6D_6) δ 153.7 (s). ^{13}C{^{1}H} NMR (62.8 MHz, $CDCl_3$) δ 215.6 (s, CO), 201.2 (d, C$_\beta$, $^3J_{P-C}$ = 10.8 Hz), 140.1 (d, C$_i$, $^1J_{P-C}$ = 29.5 Hz), 136.9 (s, C$_i$″) 135.8 (d, C$_o$, $^2J_{P-C}$ = 7.7 Hz), 133.7 (d, C$_i$′, $^1J_{P-C}$ = 29 Hz), 133.3 (d, C$_o$′, $^2J_{P-C}$ = 8.2 Hz), 129.8 (s, C$_o$″), 129.1 (s, C$_p$″), 128.9 (s, C$_p$′, C$_p$″), 127.7 (d, C$_m$, C$_m$′, $^3J_{P-C}$ = 10.8 Hz), 124.9 (s, C$_m$″), 78.7 (d, C$_\alpha$, $^2J_{P-C}$ = 42.5 Hz), 56.3 (s, Cy-*C*N), 33.1 (s, Cy-*C*H$_2$), 24.8 (s, Cy-*C*H$_2$), 24.2 (s, Cy-CH$_2$).

Synthesis of $Ru_2(CO)_6[\mu$-C{NH(Cy)}CH(Ph)](μ-PPh$_2$) (3b). Complex **1b** (R = Ph; 0.50 g, 0.76 mmol) was dissolved in 25 mL of heptane and 5 mL of toluene. An excess of cyclohexylamine (0.5 mL, 4.37 mmol) was added to the briskly stirred solution. The yellow solution became almost colorless, and the stirring was stopped. The solution was allowed to stand for 24 h. At the end of that time, pale yellow crystals of product had precipitated onto the walls of the Schlenk tube. The supernatant was decanted off, and the crystals were washed with pentane and dried in vacuo. The isolated yield of **3b** was 0.496 g (86%). Anal. Calcd for $C_{32}H_{28}NO_6PRu_2{\cdot}C_6H_{12}$: C, 54.34; H, 4.80; N, 1.67; P, 3.69. Found: C, 54.18; H, 4.35; N, 1.78; P, 3.93. IR (C_6H_{12}) ν(CO) 2064 s, 2033 vs, 1995 s, 1977 s, 1960 m cm^{-1}; (Nujol mull) ν(N–H) 3270 w cm^{-1}, ν(C=N) 1528 cm^{-1}. ^{1}H NMR (250 MHz, $CDCl_3$) δ 7.67 (m, Ph-*H*), 7.18 (m, Ph-*H*), 6.99 (m, Ph-*H*), 6.47 (d, N*H*, $^3J_{H-H}$ = 7.1 Hz), 4.19 (m, NC*H*), 2.50 (d, C$_\beta$*H*, $^3J_{P-H}$ = 12.2 Hz), 2.0–0.8 (m, Cy-CH$_2$). ^{31}P{^{1}H} NMR 101.3 MHz, $CDCl_3$) δ 155.0 (s). ^{13}C{H} NMR (62.8 MHz, $CDCl_3$) δ 227.4 (d, C$_\alpha$, $^2J_{P-C}$ = 7.4 Hz), 203.3 (d, CO(2), $^2J_{P-C}$ = 62.8 Hz), 202.4 (d, CO(5), $^2J_{P-C}$ = 53.6 Hz), 198.9 (d, CO(3), $^2J_{P-C}$ = 12.0 Hz), 198.8 (d CO(6), $^2J_{P-C}$ = 10.5 Hz), 196.7 (d, CO(4), $^2J_{P-C}$ = 2.5 Hz), 196.3 (d, CO(1), $^2J_{P-C}$ = 4 Hz), 145.7 (d, C$_i$″, $^3J_{P-C}$ = 7.6 Hz), 141.3 (d, C$_i$, $^1J_{P-C}$ = 32.8 Hz), 136.8 (d, C$_i$′, $^1J_{P-C}$ = 24.0 Hz), 134.6 (d, C$_o$, $^2J_{P-C}$ = 9.1 Hz), 133.7 (d, C$_o$′, $^2J_{P-C}$ = 10.5 Hz), 129.5 (s, C$_p$), 129.3 (s, C$_p$′), 129.1 (s, C$_o$″), 128.3 (d, C$_m$, $^3J_{P-C}$ = 10.5 Hz), 128.2 (d, C$_m$′, $^3J_{P-C}$ = 12.4 Hz), 126.7 (s, C$_m$″), 124.7 (s, C$_p$″), 60.3 (s, Cy-*C*N); 42.6 (d, C$_\beta$, $^2J_{P-C}$ = 5.3 Hz), 33.6 (s, Cy-*C*H$_2$), 31.4 (s, Cy-*C*H$_2$), 25.1 (s, Cy-*C*H$_2$″), 25.0 (s, Cy-*C*H$_2$‴), 24.9 (s, Cy-CH$_2$⁗).

Synthesis of $Os_2(CO)_6[\mu$-C{NH(Cy)}CH(Ph)](μ-PPh$_2$) (3c). In a reaction similar to the formation of **3b** above, 0.19 g (0.22 mmol) of **1c** was dissolved in 10 mL of hexane and 2 mL of toluene. Cyclohexylamine (0.2 mL, 1.75 mmol) was added to the colorless solution, which became bright yellow before fading to pale yellow in 30 s. After standing for 24 h, the supernatant was decanted from the pale yellow crystals, the crystals washed with pentane and dried in vacuo. The isolated yield of **3b** was 0.17 g (78.5%). Anal. Calcd for $C_{32}H_{28}NO_6Os_2P$: C, 41.15; H, 3.02; P, 3.32; N, 1.50. Found: C, 41.03; H, 2.90; P, 3.16; N, 1.55. IR (C_6H_{12}) ν(CO) 2064 s, 2032 vs, 1989 s, 1965 vs, 1950 m cm^{-1}; (Nujol mull) ν(N–H) 3273 w cm^{-1}, ν(C=N) 1535 m cm^{-1}. ^{1}H NMR (250 MHz, $CDCl_3$) δ 7.72 (m, Ph-*H*), 7.45–6.87 (m, Ph-H), 6.48 (br s, N*H*), 4.18 (m, NC*H*), 2.44 (dd, C$_\beta$-*H*, $^3J_{P-H}$ = 15.4 Hz, $^4J_{H-H}$ = 1.5 Hz), 2.08–0.96 (m, Cy-CH_2). ^{31}P{^{1}H} NMR (101.3 MHz, $CDCl_3$) δ 84.7 (s). ^{13}C{^{1}H} NMR (65.8 MHz, $CDCl_3$) δ 207.2 (d, C$_\alpha$, $^2J_{P-C}$ = 3.7 Hz), 186.1 (d, CO(2), $^2J_{P-C}$ = 59.3 Hz), 184.5 (d, CO(5), $^2J_{P-C}$ = 52.9 Hz), 180.1 (d, CO(3), $^2J_{P-C}$ = 8.0 Mz), 178.7 (d, CO(6), $^2J_{P-C}$ = 7.0 Hz), 177.9 (s, CO(4)), 176.9 (d, CO(1), $^2J_{P-C}$ = 3.8 Hz), 146.5 (d, C$_i$″, $^3J_{P-C}$ = 7.9 Hz), 139.1 (d, C$_i$, $^1J_{P-C}$ = 45.4 Hz), 135.3 (d, C$_o$, $^2J_{P-C}$ = 9.9 Hz), 134.5 (d, C$_o$′, $^2J_{P-C}$ = 10.9 Hz), 133.0 (d, C$_i$′, $^1J_{P-C}$ = 36.0 Hz), 129.8 (s, C$_o$″), 129.1 (s, C$_p$, C$_p$′), 128.8 (d, C$_m$, $^3J_{P-C}$ = 10.0 Hz), 128.4 (d, C$_m$, $^3J_{P-C}$ = 11.1 Hz), 126.9 (s, C$_m$″), 125.1 (s, C$_p$″), 61.1 (s, Cy-*C*N), 33.6 (s, Cy-*C*H$_2$), 31.3 (s, Cy-*C*H$_2$′), 31.1 (s, C$_\beta$), 25.1 (s, Cy-CH$_2$″), 24.9 (s, Cy-CH$_2$‴), 24.8 (s, Cy-CH$_2$⁗).

Synthesis of $Ru_2(CO)_6[\mu$-C{NH(*i*-Pr)}CH(Ph)](μ-PPh$_2$) (5b). From 0.62 g (0.944 mmol) of **1b**, with excess isopropylamine was obtained 0.54 g (81%) of **5a** in a procedure similar to the production of **3b**. Anal. Calcd for $C_{29}H_{23}NO_6PRu_2$: C, 48.74; H, 3.24; N, 1.96; P, 4.33. Found: C, 48.72; H, 3.40; N, 2.08; P, 4.14. IR (C_6H_{12}) ν(CO) 2063 s, 2033 vs, 1996 s, 1978 s, 1961 m cm^{-1}; (Nujol mull) ν(NH) 3272 w cm^{-1}, ν(C=N) 1527 m cm^{-1}. ^{1}H NMR (250 MHz, $CDCl_3$) δ 7.75 (m, Ph-*H*), 7.34–6.91 (m, Ph-*H*), 6.55 (br d, N*H*, $^3J_{H-H}$ = 6.8 Hz), 4.66 (m, *i*-Pr-C*H*, $^3J_{H-H'}$ = 9.9 Hz, $^3J_{H-H}$ = 6.4 Hz), 2.57 (d, C$_\beta$*H*, $^3J_{P-H}$ = 13.3 Hz), 1.33 (d, CH_3, $^3J_{H-H}$ = 6.4 Hz), 1.10 (d, CH_3′, $^3J_{H-H}$ = 6.4 Hz). ^{31}P{^{1}H} NMR (101.3 MHz, $CDCl_3$) δ 155.9 (s). ^{13}C{^{1}H} NMR (62.8 MHz, $CDCl_3$) δ 227.3 (s, C$_\alpha$), 203.3 (d, CO, $^2J_{P-C}$ = 60.0 Hz), 202.8 (d, CO, $^2J_{P-C}$ = 53.3 Hz), 198.8 (d, CO, $^2J_{P-C}$ = 11.9 Hz), 198.6 (d, CO, $^2J_{P-C}$ = 11.0 Hz), 196.6 (s, CO), 196.2 (s, CO), 145.6 (d, C$_i$″, $^3J_{P-C}$ = 7.6 Hz), 141.3 (d, C$_i$, $^1J_{P-C}$ = 32.6 Hz), 136.8 (d, C$_i$′, $^1J_{P-C}$ = 24.5 Hz), 134.6 (d, C$_o$, $^2J_{P-C}$ = 9.4 Hz), 133.6 (d, C$_o$′, $^2J_{P-C}$ = 9.7 Hz), 129.4 (s, C$_p$), 129.2 (s, C$_p$′), 129.0 (s, C$_o$′), 128.3 (d, C$_m$, $^3J_{P-C}$ = 12.4 Hz), 128.1 (d, C$_m$′, $^3J_{P-C}$ = 10.1 Hz), 126.7 (s, C$_m$″), 124.7 (s, C$_p$″), 53.0 (s, *i*-Pr-*C*H), 42.6 (d, C$_\beta$, $^2J_{P-C}$ = 4.6 Hz), 23.0 (s, *C*H$_3$), 20.7 (s, *C*H$_3$′).

Synthesis of $Os_2(CO)_6[\mu$-C{NH(*i*-Pr)}CH(Ph)](μ-PPh$_2$) (5c). The procedure was similar to the synthesis of **3c**, using excess isopropylamine in place of cyclohexylamine. The reaction of 0.314 g of **1c** yielded 0.25 g (75%) of **5b**. Anal. Calcd for $C_{29}H_{23}NO_6Os_2P{\cdot}0.33C_6H_{12}$: C, 40.43; H, 2.96; N, 1.52; P, 3.36. Found: C, 40.09; H, 2.99; N, 1.49; P, 3.70. IR (C_6H_{12}) ν(CO) 2066 s, 2033 vs, 1991 s, 1967 vs, 1951 m, cm^{-1}; (Nujol mull) ν(N–H) 3274 w cm^{-1}, ν(C=N) 1538 m cm^{-1}. ^{1}H NMR (250 MHz, $CDCl_3$) 7.77 (m, Ph-*H*), 7.53–6.94 (m, Ph-*H*), 6.51 (br, s, N*H*), 4.65 (m, *i*-Pr-C*H*, $^3J_{H-H}$ = 9.9 Hz, $^3J_{H-H'}$ = 6.5 Hz), 2.51 (d, C$_\beta$*H*, $^3J_{P-H}$ = 15.3 Hz), 1.35 (d, CH_3, $^3J_{P-H}$ = 6.5 Hz), 1.13 (d, CH_3′, $^3J_{H-H}$ = 6.5 Hz). ^{31}P{^{1}H} NMR (101.3 MHz, $CDCl_3$) δ 84.7 (s). ^{13}C{^{1}H} NMR (62.8 MHz, $CDCl_3$) δ 207.1 (d, C$_\alpha$, $^2J_{P-C}$ = 3.3 Hz), 186.0 (CO, $^2J_{P-C}$ = 60.0 Hz), 184.4 (d, CO, $^2J_{P-C}$ = 48.0 Hz), 180.0 (d, CO, $^2J_{P-C}$ = 7.3 Hz), 178.6 (s, CO), 177.9 (s, CO), 176.8 (s, CO), 146.4 (d, C$_i$″, $^3J_{P-C}$ = 7.5 Hz), 139.0 (d, C$_i$, $^1J_{P-C}$ = 44.9 Hz), 135.3 (d, C$_o$, $^2J_{P-C}$ = 9.8 Hz), 134.4 (d, C$_o$′, $^2J_{P-C}$ = 11.0 Hz), 132.9 (d, C$_i$′, $^1J_{P-C}$ = 34.8 Hz), 129.7 (s, C$_p$ + C$_p$′), 129.1 (s, C$_o$′), 128.7 (d, C$_m$, $^3J_{P-C}$ = 9.2 Hz), 128.4 (d, C$_m$′, $^2J_{P-C}$ = 10.6 Hz), 126.8 (s, C$_m$″), 125.1 (s, C$_p$′), 54.0 (s, *i*-Pr-*C*H), 31.0 (s, C$_\beta$), 23.2 (s, CH$_3$), 20.8 (s, CH$_3$′).

Synthesis of $Os_2(CO)_6[\mu$-C{NH(*i*-Pr)}CHPh](μ-PPh$_2$) (6). Serendipitously in the preparation of **5c** a pale yellow precipitate dropped out of solution. The IR and ^{1}H, ^{31}P{^{1}H}, and ^{13}C{^{1}H} NMR spectra were measured and are consistent with the formulation **6**; on standing, this precipitate is converted to **5c**. IR (C_6H_{12}) ν(CO) 2065 vs, 2032 vs, 1995 vs, 1967 s, 1946 m cm^{-1}. ^{1}H NMR (250 MHz, $CDCl_3$) δ 7.83 (m, Ph-*H*), 7.77 (m, Ph-*H*), 7.66–6.80 (*m*-Ph-*H*), 6.20 (d, N*H*, $^3J_{H-H}$ = 7.2 Hz), 4.18 (d, C$_\beta$*H*, $^3J_{P-C}$ = 14.8 Hz), 4.04 (m, *i*-Pr-C*H*, $^3J_{H-H}$ = 6.6 Hz), 1.05 (d, CH$_3$, $^3J_{H-H}$ = 6.5 Hz), 0.65 (d, CH$_3^1$, $^3J_{H-H}$ = 6.4 Hz). ^{31}P{^{1}H} (101.3 MHz, $CDCl_3$) 67.8 (s). ^{13}C{^{1}H} NMR (62.8 MHz, $CDCl_3$), 222.4 (s, C$_\alpha$), 187.5 (s, CO), 187.0 (d, CO, $^2J_{P-C}$ = 34.3 Hz), 186.3 (s, CO), 178.9 (d, CO, $^2J_{P-C}$ = 24.4 Hz), 178.8 (s, CO), 178.2 (d, CO, $^2J_{P-C}$ = 10.1 Hz), 148.2 (s, C$_i$″), 141.5 (d, C$_i$, $^1J_{P-C}$ = 43.9 Hz), 135.4 (d, C$_i$′, $^1J_{P-C}$ = 32.6 Hz), 134.9 (d, C$_o$, $^2J_{P-C}$ = 11.3 Hz), 133.7 (d, C$_o$′, $^2J_{P-C}$ = 11.3 Hz), 129.8 (s, C$_p$), 129.5 (s, C$_p$′), 128.9 (d, C$_m$, $^3J_{P-C}$ = 9.7 Hz), 128.8 (s, C$_o$″), 128.3 (d, C$_m$′, $^3J_{P-C}$ = 11.0 Hz), 126.3 (s, C$_m$″), 124.6 (s, C$_p$″), 124.6

(13) Benn, R.; Gunther, H.; *Angew. Chem., Int. Ed. Engl.* **1983**, *22*, 350.

Table I. Summary of Crystal Data, Intensity Collection, Reduction, and Refinement for Compounds $M_2(CO)_6[\mu_2\text{-}C\{NH(Cy)\}CH(Ph)](\mu\text{-}PPh_2)$ (M = Ru, 3b; M = Os, 3c)

	3b	3c
formula	$Ru_2PO_6NC_{32}H_{28}\cdot 0.5C_7H_8$	$Os_2PO_6NC_{32}H_{28}\cdot 0.5C_7H_8$
mol wt	801.77	980.0
cryst syst	monoclinic	monoclinic
a, Å	10.076 (3)	10.164 (2)
b, Å	17.290 (4)	17.126 (5)
c, Å	20.807 (4)	20.691 (5)
β, deg	102.18 (2)	99.44 (2)
Z	4	4
V, Å^3	3543.3 (15)	3552.9 (15)
d_{calcd}, g cm^{-3}	1.503	1.832
$F(000)$	1608	1864
μ(Mo Kα), cm^{-1}	9.24	76.90
radiation	graphite-monochromated Mo Kα (λ = 0.71073 Å)	
temp, K	294 ± 1	294 ± 1
diffractometer	Syntex $P2_1$	Syntex $P2_1$
cryst size, mm	0.26 × 0.27 × 0.30	0.16 (±2) spherical
scan type	$\theta/2\theta$	$\theta/2\theta$
2θ range, deg	3.2–48.0	3.2–48.0
scan speed	variable 2.93–29.3° min^{-1}	
scan width	0.8° below Kα_1 to 0.8° above Kα_2	
std reflns	093; 541	145; 354
change in standards, %	−5	−7
data measd	5597	5625
data obsd ($I > 3\sigma(I)$)	4372	4051
transm factors	0.72–0.82	0.37–0.46
no. of variables	519	407
$R = \sum(\|F_o\| - \|F_c\|)/\sum\|F_o\|$	0.030	0.035
$R_w = [\sum w(\|F_o\| - \|F_c\|)^2/\sum\|F_o\|^2]^{1/2}$	0.035	0.038
weighting scheme	$1.9 - 0.015\|F_o\| + 0.0002\|F_o\|^2$	$1.75 - 0.0119\|F_o\| + 0.00006\|F_o\|^2$
residual electron density, e Å^{-3}	0.4	0.75

(s, C_p''), 51.5 (s, *i*-Pr-*C*H), 22.8 (s, *C*H$_3$), 19.9 (s, *C*H$_3'$), 19.9 (s, C_β).

X-ray Structural Analysis of 3b and 3c. Crystals of **3b** and **3c** were both grown from heptane/toluene mixtures at −5 °C as pale yellow prisms. Experimental details of data collection, reduction, and refinement are given in Table I. Since procedures were similar in both cases, a description is given for **3b** only. An appropriate crystal was chosen, affixed to a glass fiber with epoxy glue, and mounted on a goniometer head with a brass pin. The data crystals of both **3b** and **3c** were coated with epoxy cement to prevent loss of toluene solvate during data collection. The Syntex $P2_1$ diffractometer is controlled by a Data General Nova computer. Preliminary measurements on the diffractometer using the Syntex polaroid rotation photography, autoindexing, and cell refinement routines were used to define a unit cell and space group. Accurate unit cell dimensions were obtained from least-squares fitting of 2θ, ω, and χ values for 15 reasonably intense reflections well distributed in reciprocal space. Refined values are listed in Table I. As the data indicate, **3b** and **3c** are isomorphous. They are also isomorphous with **3a**.[7e]

Intensity data were collected at 294 ± 1 K using a coupled θ (crystal)–2θ (counter) scan with a scan rate set to optimize measurements for weak and strong reflections. Background counts were measured at the beginning and end of each scan for half of the total scan time. Standard reflections were monitored after every 100 measurements and used to scale the data to a common level. Lorentz and polarization corrections were applied to all data. A spherical absorption correction was applied to **3c** (μ = 76.90 cm^{-1}) but not to **3b** (μ = 9.24 cm^{-1}).

The structure of **3b** was solved by the heavy-atom method, which revealed positions for the two metal and phosphorus atoms. Subsequent Fourier syntheses defined light-atom positions, and hydrogen atoms were located in **3b** via a difference Fourier map in the final stages of refinement. Both structures were found to contain disordered toluene solvate molecules about the inversion center at 001/2. The toluene methyl group was not locatable in either case and is presumed to be disordered over all six possible sites. In the last cycles of refinement, all nonsolvent hydrogen atoms were included with positions and isotropic temperature factors varying. A final difference map had residual electron density at the level of 0.4 e Å^{-3} and was featureless.

Table II. Atomic Positions (Fractional × 10^4) for $Ru_2(CO)_6[\mu_2\text{-}C\{NH(Cy)\}CH(Ph)](\mu\text{-}PPh_2)$ (3b)

atom	x	y	z
Ru(1)	3866.8 (3)	389.3 (2)	1056.2 (2)
Ru(2)	1466.0 (3)	634.9 (2)	1492.4 (2)
P	3176.6 (11)	−240.2 (6)	1935.8 (5)
O(1)	6947 (4)	231 (2)	1274 (2)
O(2)	3171 (4)	1289 (2)	−227 (2)
O(3)	3056 (5)	−1068 (2)	224 (2)
O(4)	−323 (4)	795 (3)	2493 (2)
O(5)	449 (4)	1889 (2)	465 (2)
O(6)	−269 (4)	−579 (2)	636 (2)
N	4468 (4)	2094 (2)	1462 (2)
C(1)	5793 (5)	276 (3)	1192 (2)
C(2)	3440 (5)	971 (3)	255 (2)
C(3)	3388 (5)	−546 (3)	547 (2)
C(4)	343 (5)	745 (3)	2118 (2)
C(5)	800 (5)	1434 (3)	855 (3)
C(6)	388 (5)	−137 (3)	962 (2)
C(7)	3895 (4)	1438 (2)	1578 (2)
C(8)	2994 (4)	1453 (2)	2047 (2)
C(9)	5384 (5)	2248 (3)	1010 (3)
C(10)	6764 (7)	2477 (4)	1400 (4)
C(11)	7760 (9)	2643 (7)	954 (6)
C(12)	6993 (14)	3200 (6)	387 (7)
C(13)	5616 (12)	3004 (5)	9 (5)
C(14)	4739 (9)	2866 (3)	505 (4)
C(15)	2563 (4)	2204 (2)	2303 (2)
C(16)	2655 (5)	2272 (3)	2977 (3)
C(17)	2283 (6)	2957 (4)	3251 (3)
C(18)	1798 (6)	3569 (4)	2854 (4)
C(19)	1680 (6)	3514 (3)	2186 (4)
C(20)	2052 (5)	2834 (3)	1913 (3)
C(21)	2908 (4)	−1284 (2)	1886 (2)
C(22)	3939 (5)	−1787 (3)	1807 (3)
C(23)	3686 (6)	−2585 (3)	1754 (3)
C(24)	2447 (6)	−2873 (3)	1796 (4)
C(25)	1430 (6)	−2388 (3)	1893 (4)
C(26)	1667 (5)	−1590 (3)	1942 (3)
C(27)	4152 (4)	−133 (2)	2779 (2)
C(28)	5549 (5)	−133 (3)	2908 (2)
C(29)	6299 (6)	−24 (4)	3547 (3)
C(30)	5632 (8)	80 (3)	4055 (3)
C(31)	4264 (8)	79 (4)	3929 (3)
C(32)	3502 (6)	−40 (3)	3295 (2)
C(33)[a]	234 (17)	−129 (20)	4501 (10)
C(34)[a]	535 (19)	817 (18)	4466 (13)
C(35)[a]	390 (23)	771 (16)	5152 (19)

[a] Solvent.

For **3c** the atom coordinates of **3b** were used as a starting point for refinement. Hydrogen atoms were not included.

All calculations were carried out on linked IBM 4341 systems in the Department of Computer Services at the University of Waterloo using a program package described elsewhere.[7e] The full matrix was employed in all least-squares refinements, and scattering factors, including corrections for anomalous dispersion for heavy atoms, were taken from ref 14.

Positional parameters for **3b** and **3c** are given in Tables II and III, and a comparison of bond lengths and angles is in Table IV. Thermal parameters (Tables S1 and S2), remaining bond lengths and angles (Table S3), and structure factors (Tables S4 and S5) have been deposited as supplementary material (see paragraph at the end of the paper).

Results and Discussion

Synthetic Aspects. As previously described for **1a**,[7e,f] primary amines give two possible addition products, a

(14) (a) *International Tables for X-ray Crystallography*; Kynoch Press: Birmingham, 1974; Vol. IV. (b) Stewart, R. F.; Davidson, E. R.; Simpson, W. T. *J. Chem. Phys.* **1965**, *42*, 3175.

Table III. Atomic Positions (Fractional × 10^4) for $Os_2(CO)_6[\mu_2$-C{NH(Cy)CH(Ph)}$](\mu$-$PPh_2)$ (3c)

atom	x	y	z
Os(1)	3831.0 (4)	391.4 (2)	1022.1 (2)
Os(2)	1385.1 (4)	629.5 (2)	1468.5 (2)
P	3059.2 (25)	-256.8 (14)	1899.2 (12)
O(1)	6848 (7)	163 (5)	1216 (4)
O(2)	3307 (10)	1373 (6)	-218 (4)
O(3)	3041 (11)	-1057 (5)	185 (4)
O(4)	-486 (9)	804 (6)	2467 (5)
O(5)	509 (9)	1909 (5)	460 (4)
O(6)	-317 (9)	-571 (5)	621 (4)
N	4446 (8)	2097 (4)	1475 (4)
C(1)	5728 (11)	251 (6)	1148 (5)
C(2)	3528 (12)	1006 (7)	245 (5)
C(3)	3331 (12)	-535 (6)	500 (5)
C(4)	223 (10)	730 (6)	2085 (5)
C(5)	784 (11)	1432 (7)	841 (6)
C(6)	326 (10)	-140 (7)	939 (5)
C(7)	3859 (9)	1441 (5)	1566 (4)
C(8)	2882 (9)	1443 (5)	2033 (5)
C(9)	5497 (12)	2230 (7)	1073 (6)
C(10)	6865 (13)	2327 (11)	1569 (9)
C(11)	7979 (20)	2472 (14)	1133 (13)
C(12)	7559 (35)	3111 (13)	685 (16)
C(13)	6272 (33)	3096 (13)	196 (13)
C(14)	5093 (21)	2926 (8)	643 (10)
C(15)	2468 (10)	2223 (6)	2299 (5)
C(16)	2584 (11)	2271 (8)	2973 (5)
C(17)	2231 (14)	2976 (9)	3263 (7)
C(18)	1783 (13)	3599 (9)	2879 (9)
C(19)	1643 (13)	3552 (7)	2195 (9)
C(20)	1980 (12)	2845 (6)	1891 (7)
C(21)	2838 (10)	-1311 (6)	1829 (5)
C(22)	3924 (11)	-1794 (6)	1747 (6)
C(23)	3741 (14)	-2599 (7)	1695 (7)
C(24)	2463 (14)	-2926 (8)	1730 (8)
C(25)	1415 (13)	-2446 (7)	1798 (8)
C(26)	1597 (12)	-1632 (6)	1862 (6)
C(27)	3945 (10)	-144 (5)	2741 (4)
C(28)	5325 (12)	-157 (7)	2864 (6)
C(29)	6032 (14)	-37 (8)	3501 (7)
C(30)	5296 (16)	103 (7)	4008 (7)
C(31)	3935 (17)	103 (8)	3877 (6)
C(32)	3222 (13)	-22 (7)	3253 (5)
C(33)[a]	-231 (42)	-752 (25)	5419 (21)
C(34)[a]	30 (36)	61 (28)	5653 (17)
C(35)[a]	913 (31)	617 (32)	5312 (18)

[a] Solvent.

one-carbon-bridged μ-alkylidene complex (**4a**) or a two-carbon-bridged 2-amino-1-metallaphenethylidene zwitterionic product (**3a**). ^{31}P NMR studies[7f] indicate that **3a** and **4a** are formed by distinct pathways with μ-η-vinylidene and μ-η^2-enamine intermediates involved en route to **4a** but with no detectable intermediates between **1a** and **3a**. In contrast for **1b** and **1c** only the single, two-carbon-bridged 2-amino-1-metallaphenethylidene products **3b** and **3c** are formed. More detailed examination of the reaction of isopropylamine with **1c** and **1b** provided further insight. A pale yellow solid precipitating early from solutions used in the preparation of **5c** has both a nitrogen proton *and* a vinyl proton in its ^1H NMR spectrum. This species has a ^{31}P shift of 67.8 ppm and is presumed to be the enamine **6**.[15] Monitoring the reaction of **1b** with isopropylamine by ^{31}P NMR at 268 K identified first a short-lived intermediate **7b** (177.9 ppm) and a much longer lived species (140.9 ppm) that converts cleanly to the final product **3b** (Figure 1). These results are consistent with the reaction pathway illustrated in Scheme III. Initial attack at the α-carbon atom of **1b** or **1c** generates the ammonium adduct

(15) An alternative structure for **6** is an isomer of **3b** in which the phenyl group on C_β faces the phosphido bridge. If this is the kinetic product of proton transfer it rapidly isomerizes to the final thermodynamic species **3b**.

Table IV. Bond Lengths (Å) and Angles (deg) for 3b and 3c

	M = Ru	M = Os
	Bond Lengths	
M(1)-M(2)	2.7896 (4)	2.8197 (5)
M(1)-P	2.357 (1)	2.368 (2)
M(2)-P	2.333 (1)	2.344 (2)
M(1)-C(1)	1.912 (5)	1.918 (11)
M(1)-C(2)	1.916 (5)	1.903 (11)
M(1)-C(3)	1.939 (5)	1.939 (11)
M(2)-C(4)	1.906 (5)	1.883 (11)
M(2)-C(5)	1.934 (5)	1.902 (12)
M(2)-C(6)	1.916 (5)	1.926 (11)
M(1)-C(7)	2.110 (4)	2.118 (9)
M(2)-C(8)	2.225 (4)	2.243 (9)
P-C(21)	1.825 (4)	1.822 (10)
P-C(27)	1.831 (4)	1.836 (10)
C(1)-O(1)	1.141 (6)	1.133 (14)
C(2)-O(2)	1.126 (6)	1.137 (14)
C(3)-O(3)	1.131 (6)	1.117 (14)
C(4)-O(4)	1.136 (7)	1.160 (14)
C(5)-O(5)	1.132 (6)	1.138 (15)
C(6)-O(6)	1.137 (6)	1.124 (14)
C(7)-C(8)	1.468 (5)	1.496 (13)
C(7)-N	1.318 (5)	1.299 (12)
C(8)-C(15)	1.502 (6)	1.530 (14)
N-C(9)	1.474 (6)	1.474 (15)
	Bond Angles	
M(2)-M(1)-P	53.09 (2)	52.85 (6)
M(2)-M(1)-C(1)	153.0 (1)	153.4 (3)
M(2)-M(1)-C(2)	98.8 (1)	99.6 (3)
M(2)-M(1)-C(3)	99.9 (1)	97.8 (3)
M(2)-M(1)-C(7)	67.7 (1)	68.9 (2)
P-M(1)-C(1)	107.2 (1)	106.8 (3)
P-M(1)-C(2)	150.3 (1)	151.4 (3)
P-M(1)-C(3)	87.7 (1)	87.4 (3)
P-M(1)-C(7)	88.4 (1)	88.2 (3)
C(1)-M(1)-C(2)	102.5 (2)	101.8 (5)
C(1)-M(1)-C(3)	97.1 (2)	98.0 (5)
C(1)-M(1)-C(7)	96.3 (2)	96.2 (4)
C(2)-M(1)-C(3)	88.7 (2)	89.4 (5)
C(2)-M(1)-C(7)	88.4 (2)	88.1 (4)
C(3)-M(1)-C(7)	166.7 (2)	165.8 (4)
M(1)-M(2)-P	53.90 (2)	53.63 (6)
M(1)-M(2)-C(4)	156.6 (1)	156.9 (3)
M(1)-M(2)-C(5)	94.9 (1)	94.7 (3)
M(1)-M(2)-C(6)	97.6 (1)	98.9 (3)
M(1)-M(2)-C(8)	73.3 (1)	72.6 (2)
P-M(2)-C(4)	106.9 (1)	107.4 (3)
P-M(2)-C(5)	148.8 (1)	148.3 (3)
P-M(2)-C(6)	93.3 (1)	94.4 (3)
P-M(2)-C(8)	80.5 (1)	79.4 (2)
C(4)-M(2)-C(5)	103.1 (2)	103.2 (5)
C(4)-M(2)-C(6)	96.7 (2)	95.4 (4)
C(4)-M(2)-C(8)	91.6 (2)	92.2 (4)
C(5)-M(2)-C(6)	91.7 (2)	91.0 (5)
C(5)-M(2)-C(8)	90.2 (2)	91.3 (4)
C(6)-M(2)-C(8)	170.9 (2)	171.4 (4)
M(1)-P-M(2)	73.00 (2)	73.52 (6)
M(1)-P-C(21)	118.5 (1)	117.1 (3)
M(1)-P-C(27)	120.7 (1)	120.4 (3)
M(2)-P-C(21)	122.1 (1)	122.6 (3)
M(2)-P-C(27)	121.1 (1)	120.4 (3)
C(21)-P-C(27)	101.4 (2)	102.4 (4)
M(1)-C(1)-O(1)	178.0 (2)	179.2 (4)
M(1)-C(2)-O(2)	177.5 (2)	178.0 (5)
M(1)-C(3)-O(3)	176.0 (2)	178.2 (5)
M(2)-Cn4)-O(4)	178.6 (2)	179.0 (5)
M(2)-C(5)-O(5)	176.8 (2)	175.6 (5)
M(2)-C(6)-O(6)	178.1 (2)	177.9 (5)
M(1)-C(7)-C(8)	114.5 (1)	113.1 (3)
M(1)-C(7)-N	127.2 (1)	128.5 (3)
C(8)-C(7)-N	117.6 (2)	117.5 (5)
M(2)-C(8)-C(7)	95.8 (1)	97.3 (3)
M(2)-C(8)-C(15)	120.9 (2)	121.8 (4)
C(7)-C(8)-C(15)	121.1 (2)	119.0 (5)
C(7)-N-C(9)	129.0 (3)	127.4 (6)

7, a short-lived intermediate, which undergoes proton transfer to the β-carbon to give the longer lived enamine

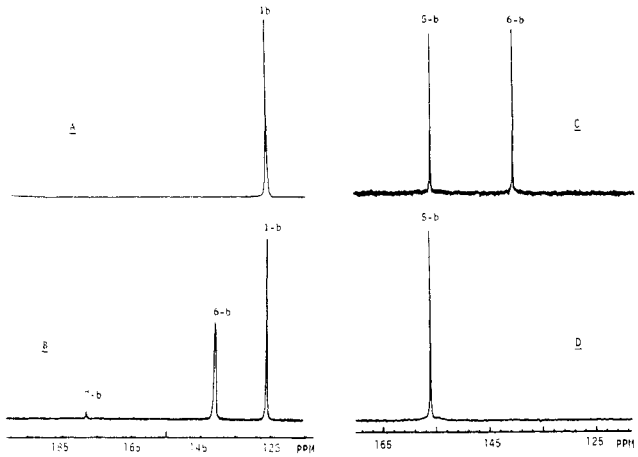

Figure 1. Reaction of **1b** with isopropylamine followed by $^{31}P\{^1H\}$ NMR at 268 K (101.3 MHz) in $CDCl_3$ showing (A) the initial presence of **1b** (130.5 ppm), (B) the short-lived intermediate **7b** (177.9 ppm) and the longer lived enamine intermediate **6b** (140.9 ppm), (C) the conversion of **6b** to the final product **5b** (155.9 ppm), (D) **5b**.

Scheme III

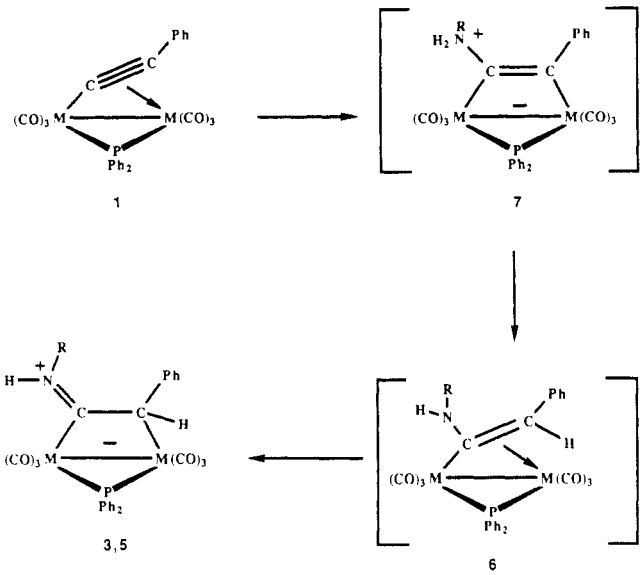

6. Valence isomerization of the latter affords the final, thermodynamically stable isomer **3**. There is ample precedent for **7**, in the structural characterization of adducts at C_α with other nucleophiles.[7b,i] Although an enamine complex of type **6** has not been structurally characterized, analogous binuclear σ–π-vinyl species are well-known.[16] It is of interest to note the changing pattern of reactivity down the triad. With primary amines **1a** affords both α- and β-adducts while **1b** and **1c** yield only α-addition products. For secondary amines **1a** gives uniquely β-addition, whereas the ruthenium and osmium complexes show a much greater propensity for α-attack, the ratio of α- to β-addition being ca. 1:1. The change in product distribution down the triad for the same nucleophile appears to have its origin in orbital control of the reactions.[17] The acetylides **1** like many σ–π-bound ligands are dynamic, with the σ- and π-bound metals switching (Scheme IV).

Scheme IV. Dynamics in $M_2(CO)_6(\mu_2\text{-}\eta^2\text{-CCR})(\mu\text{-PPh}_2)$

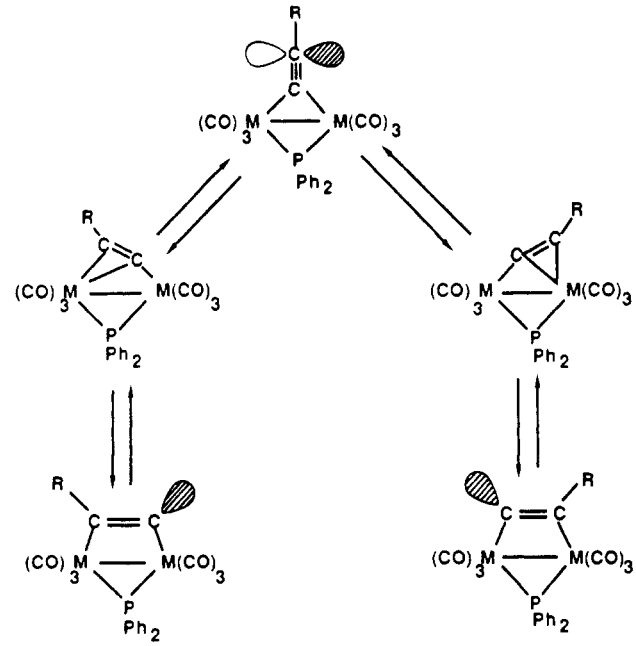

Extended Hückel molecular orbital calculations show that the LUMO has significant carbon (acetylide) character, being principally localized on C_β when the acetylide lies symmetrically perpendicular to the M–M vector (i.e., in the transition state for the fluxional process) and on C_α when the triple bond is parallel to the metal–metal bond. An increased tendency for attack at C_α down the triad is thus consistent with structural data which demonstrate that the acetylide is significantly more distorted toward the parallel configuration for M = Os.[12]

Spectroscopic Results: Infrared Spectra. The ν(CO) spectra of **3a–c**, and **5a,b** are typical of $M_2(CO)_6$ complexes with a band pattern similar to that of the precursors **1a–c** but shifted to lower frequency due to delocalization of the negative charge on the zwitterion onto the $M(CO)_3$ groups. For **3a–c** the ν(C=N) frequency *increases* by 7 cm^{-1} for each metal down the triad, indicating a strengthening of the C=N bond from Fe to Os. Although a high estimated standard deviation on the C(7)–N bond length for **3c** clouds the issue somewhat, there are indications from the X-ray data of a shortening of the C=N bond down the series.

$^{31}P\{^1H\}$ NMR Spectra. The ^{31}P chemical shifts for **3a–c** and **5b,c** (Table V) are well downfield of 85% H_3PO_4, as expected for phosphido bridges across a strong group 8 metal–metal bond[18] and 25–37 ppm downfield of the acetylides **1a–c**. Within the series of structurally related binuclear molecules $M_2(CO)_6(\mu\text{-PPh}_2)(\mu\text{-X})$, shifts in $\delta(^{31}P)$ correlate well with changes in the M–P–M angle and M–M bond length.[18a,19] In the case of **3a–c** the downfield shift implies a larger M–P–M angle and longer M–M bond than in **1a–c**, as is observed structurally. A "metal influence" on $\delta(^{31}P)$, with an upfield shift of ~20 ppm from Fe to Ru and ~70 ppm from Ru to Os for isostructural compounds is also a feature of note.

$^{13}C\{^1H\}$ NMR Spectra. There are six nonequivalent carbonyl ligands in the structures of **3a–c** (Figure 2). Accordingly six separate ^{13}CO resonances would be ex-

(16) (a) Andrianov, V. G.; Struchkov, Y. T. *J. Chem. Soc., Chem. Commun.* **1968**, 1590. (b) Dyke, A. F.; Knox, S. A. R.; Naish, P. J.; Orpen, A. G. *J. Chem. Soc., Chem. Commun.* **1980**, 441. (c) Dyke, A. F.; Knox, S. A. R.; Morris, M. J.; Naish, P. J. *J. Chem. Soc., Dalton Trans.* **1983**, 1417. (d) Casey, C. P.; Marder, S. R.; Adams, B. R. *J. Am. Chem. Soc.* **1985**, *107*, 7700.

(17) Carty, A. J.; Cherkas, A. A., manuscript in preparation.

(18) (a) Carty, A. J.; MacLaughlin, S. A.; Nucciarone, D. In *Phosphorus-31 NMR Spectroscopy in Stereochemical Analysis: Organic Compounds and Metal Complexes*; Verkade, J. G., Quinn, L. D., Eds.; VCH: New York, 1987, Chapter 16, pp 554–619. (b) Carty, A. J.; MacLaughlin, S. A.; Taylor, N. J. *J. Organomet. Chem.* **1981**, *204*, C27.

(19) Carty, A. J. *Adv. Chem. Ser.* **1982**, *196*, 163.

Table V. Selected NMR Shifts for $M_2(CO)_6(\mu\text{-}PPh_2)X$ (M = Fe, Ru, Os; X_1 = (μ_2-η^2-C≡CPh), X_2 = [μ-C{NRH}C(Ph)], X_3 = [μ-CHCNRR'(Ph)]) (J in hertz)

			$^{13}C\{^1H\}$		
	compd	$^{31}P\{^1H\}$	C_α	C_β	$^1H[H_8 (X_2); H_7 (X_3)]$
X_1	**1a**	148.3 (s)	110.0 (d, $^2J_{P-C}$ = 52.9)	91.7 (d, $^2J_{P-C}$ = 7.7)	
	1b	130.5 (s)	105.4 (d, $^2J_{P-C}$ = 27.5)	92.7 (d, $^2J_{PC}$ = 7.7)	
	1c	47.3 (s)	86.0 (d, $^2J_{P-C}$ = 19.8)	90.4 (d, $^2J_{P-C}$ = 9.3)	
X_2	**3a**	183.5 (s)	234.3 (d, $^2J_{P-C}$ = 11.2)	44.9 (d, $^2J_{P-C}$ = 3.9)	2.68 (d, $^3J_{P-H}$ = 13.0)
	3b	155.0 (s)	227.4 (d, $^2J_{P-C}$ = 7.4)	42.6 (d, $^2J_{P-C}$ = 5.3)	2.50 (d, $^3J_{P-H}$ = 12.2)
	3c	84.7 (s)	207.2 (d, $^2J_{P-C}$ = 3.7)	31.1 (s)	2.44 (dd, $^3J_{P-H}$ = 15.4)
	5b	155.9 (s)	227.3 (s)	42.6 (d, $^2J_{P-C}$ = 4.6)	2.57 (d, $^3J_{P-H}$ = 13.3, $^4J_{P-H}$ = 1.5)
	5c	84.7 (s)	207.1 (d, $^2J_{P-C}$ = 3.3)	31.0 (s)	2.51 (d, $^3J_{P-H}$ = 15.3)
	6	67.8 (s)	222.4 (s)	19.9 (s)	4.18 (d, $^3J_{P-C}$ = 14.8)
X_3	**2a**	153.9 (s)	68.1 (d, $^2J_{P-C}$ = 40.9)	198.7 (d, $^2J_{P-C}$ = 7.8)	1.62 (d, $^3J_{P-H}$ = 35.7)
	2b	136.7 (s)	55.0 (d, $^2J_{P-C}$ = 23.3)	196.0 (d, $^3J_{P-C}$ = 5.7)	1.37 (d, $^3J_{P-C}$ = 31.5)
	2c	57.6 (s)	28.8 (d, $^2J_{P-C}$ = 13.5)	196.9 (d, $^3J_{P-C}$ = 10.4)	1.44 (d, $^3J_{P-H}$ = 29.6)
	4	153.7 (s)	78.7 (d, $^2J_{P-C}$ = 42.5)	201.2 (d, $^3J_{P-C}$ = 10.8)	1.58 (d, $^3J_{P-H}$ = 34.4)

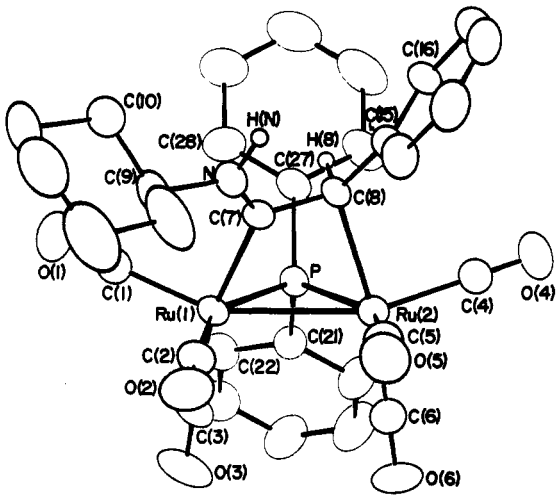

Figure 2. Ortep plot of **3b** showing the numbering scheme.

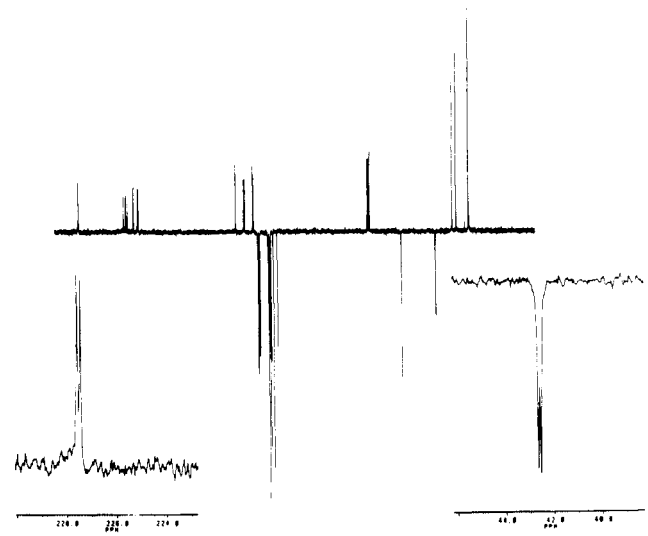

Figure 3. Spin echo ^{13}C NMR spectrum of **3b**: C, CH_2 phased up; CH, CH_3 phased down. C(7) and C(8) resonances expanded.

pected in the absence of a fluxional process equilibrating sites. For **3b** and **3c** spectra consistent with the static structure are obtained at 297 K. For example, **3b** exhibits two signals for the carbonyls trans to the phosphido bridge [C(2) and/or C(5) of Figure 2] at 203.3 and 202.4 ppm with large trans $^3J_{P-C}$ couplings of 62.8 and 53.6 Hz, respectively.[20] Two resonances for the carbonyls trans to the metal–metal bond (C(1) or C(4)) appear at 196.3 and 196.7 ppm with smaller coupling constants of 4 and 2.5 Hz to phosphorus, indicative of sites cis to the phosphido bridge. The final set of resonances due to C(3) or C(6) trans to the hydrocarbyl but cis to the phosphido bridge appear at 198.9 and 198.8 ppm with $^3J_{P-C}$ values of 12.0 and 10.5 Hz, respectively.

The remaining ruthenium and osmium complexes **3c**, **5b**, and **5c** give similar spectral results.

In the case of **3a**, the $^{13}C\{^1H\}$ NMR spectrum has four peaks, three of which can be assigned to the three CO's on M1 at 215.5, 213.9, and 211.3 ppm with coupling constants of 31.5, 0.0, and 16.4 Hz, respectively, corresponding to C(2), C(1), and C(3). The fourth broad resonance at 212.8 ppm corresponds to the three CO's on the second metal atom, which are interconverting on the NMR time scale by some dynamic process such as a trigonal rotation. Such behavior, with one $M(CO)_3$ unit static while the other is dynamic, has been observed previously for binuclear molecules including the μ-η^2-allenyl complex $Ru_2(CO)_6$-(μ_2-η^2-CH=C=CPh)(μ-PPh_2).[21]

The $^{13}C\{^1H\}$ NMR spectrum of **4**, which has a shorter M–M bond length (2.576 (1) Å) than **3a** (2.628 (1) Å) shows only one CO signal, as do the analogous $M_2(CO)_6$[μ-CHC(Ph)NEt_2](μ-PPh_2)[12] (**2a–c**), which also have shorter M–M bond lengths than their **3a–c** counterparts. In comparison, for the starting materials **1a–c** (R=*t*-Bu), which have intermediate M–M bond lengths, dynamic processes equilibrate all CO's at room temperature on the NMR time scale for **1a** (M = Fe), while **1b** (M = Ru) and **1c** (M = Os) have processes that equilibrate the two sides of the molecule but leave a distinct set of three CO signals.[11] These results suggest (i) as might be expected these dynamic processes are more facile for M = Fe and (ii) CO scrambling at a single metal site by trigonal rotation (or a related process) becomes more facile as M–M bond distance decreases in a binuclear molecule.

Since in **3a–c** C_β has a proton attached to it while C_α does not, the spin echo pulse sequence[13] was applied to unequivocally assign these resonances (Figure 3 and Table V). The C_α and C_β signals are in fact well separated, indicating a large charge separation on the hydrocarbyl fragment. Again as in the $^{31}P\{^1H\}$ spectra, there is a distinct upfield shift of $\delta(^{13}C)$ down the triad.

The ^{13}C NMR shifts for intermediate **6** lie at the two extremes for the diosmium complexes in Table V. The value of $\delta(C_\alpha)$–$\delta(C_\beta)$ (202.5 ppm) is larger than for **5c** (176.1 ppm), indicating perhaps that C_α is more electron deficient

(20) Of course we cannot unequivocally assign C(2) or C(5) since the spectroscopic results do not distinguish the two ends of the molecule. We have assumed that the larger couplings are for CO groups on M(1) for convenience.

(21) Nucciarone, D.; Taylor, N. J.; Carty, A. J. *Organometallics* **1986**, *5*, 1179.

or carbene like and that C_β has more carbon sp^3 character than in **5c**. An alternative structure to the enamine valence isomer **6** of **5c** is **8** in which C_α is represented as a carb-

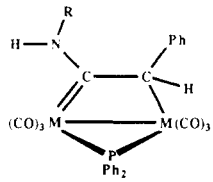

8

ene-like two-electron donor to M(1). Such a structure also gives sp^3 character to C_β. Valence isomerization to the iminium zwitterion would yield **5c**.

In the μ-alkylidene series **2a–c**, the nucleophile is attached to C_β, and the $^{13}C\{^1H\}$ NMR spectra show that in this case C_α is upfield of C_β (Table V), the reverse of that found for **3a–c** and **5a,b**. In each case however it is the atom bearing the hydrogen that is the negative end of the 1,3-dipole and hence substantially shielded.

^{1}H NMR Spectra. In the ^{1}H spectra the proton on C(8) (Figure 2) is found in the region 2.4–2.7 ppm with a slight upfield shift from Fe to Os. The resonance is coupled to phosphorus with $^3J_{P-H}$ values of 12.2–15.4 Hz. In **6** the proton resonance is at 4.18 ppm, somewhat closer to the vinylic region of 4.5–5.7 ppm.

X-ray Crystal and Molecular Structures of 3b and 3c. The two molecules **3b** and **3c** and their diiron counterpart **3a**[7e] all crystallize in the monoclinic space group $P2_1/c$. The unit cell parameters for all three compounds are very similar with the unit cell volume changing by only 117 Å^3 down the series. Thus not only are the molecules isostructural, their crystals are isomorphous. A view of a single molecule of **3b** shown in Figure 1 typifies the triad, and the same atomic numbering scheme applies to **3c**. There are no short intermolecular contacts in the crystal that are notable. Bond lengths and angles are listed in Table IV.

To facilitate delineation of structural changes down the triad, Figure 4 provides a comparison of principal skeletal parameters for the three compounds. The metal–metal distances in **3a–c** lie at the low end of the ranges for M/M single bonds between group 8 atoms[22] with the increases down the triad (Δ\{(Ru–Ru) – (Fe–Fe)\} = 0.162 Å and Δ\{(Os–Os) – (Ru–Ru)\} = 0.030 Å, reflecting the much larger difference in covalent radii between iron and ruthenium than ruthenium and osmium. The M–M distances in **3a–c** (**3a** 2.628 (1) Å; **3b** 2.7896 (4) Å; **3c** 2.8197 (5) Å) are significantly longer than in the precursors **1a–c** (R = *t*-Bu) (**1a** 2.5959 (6) Å; **1b** 2.7523 (3) Å; **1c** 2.7950 (6) Å) and longer still than in the corresponding μ-alkylidene complexes $M_2(CO)_6\{\mu$-CHC(Ph)$NEt_2\}(\mu$-$PPh_2)$ **2a–c** (**2a** 2.5477 (6) Å; **2b**, 2.7234 (4) Å; 2.7408 (8) Å), the products of β-addition, where a single-carbon bridge is present. Thus it would appear that the M–M bond in these systems is somewhat flexible, expanding with a two-carbon bridge or contracting with a single μ-alkylidene carbon bridge. Indeed it seems likely that metal–metal and metal–bridge bonding in such molecules is highly coupled with changes in the bridge influencing metal–metal interactions and vice versa. There is theoretical justification for such synergism

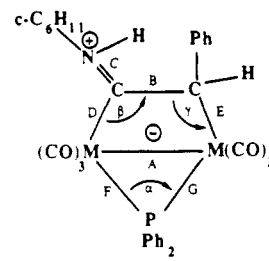

	Fe	Ru	Os
Bond Distance (Å)			
A	2.628(1)	2.7896(4)	2.8197(5)
B	1.436(10)	1.468(5)	1.496(13)
C	1.340(9)	1.318(5)	1.299(12)
D	1.999(7)	2.110(4)	2.118(9)
E	2.133(7)	2.225(4)	2.243(9)
F	2.233(2)	2.357(1)	2.368(2)
G	2.214(2)	2.333(1)	2.344(2)
Bond Angle (deg)			
α	72.50(3)	73.00(2)	73.52(6)
β	116.1(2)	114.5(1)	113.1(3)
γ	92.0(2)	95.8(1)	97.3(3)

Figure 4. Changes in important structural parameters for the series $M_2(CO)_6[\mu$-C\{NCyH\}(Ph)\}$(\mu$-$PPh_2)$ (**3a–c**).

in other bridged binuclear systems.[23] The C_α–C_β distance increases down the group as a larger M–M bond distance is spanned by the bridge. To compensate electronically the C_α–N bond lengths decrease from 1.340 (9) Å (**3a**) to 1.318 (5) Å (**3b**) to 1.299 (12) Å (M = Os) although the difference between the ruthenium and osmium compounds is not statistically significant on account of the larger esd for the C(7)–N bond length in **3c**. These C=N distances lie within the range of values found in iminium ion salts (1.28–1.38 Å).[24] The C_α–C_β bond lengths are midway between a carbon–carbon double bond (1.337 Å)[25] and a single bond between sp^2 and sp^3 hybridized carbon atoms (1.51 Å). Carbon atom C(7) has planar stereochemistry with deviations from a least-squares plane including N, C(7), Ru(1), and C(8) being +0.058 Å for **2b**. In contrast C_β is four coordinate, in a highly distorted tetrahedral environment of C(7), Ru(2), C(15), and H(8). Thus while C(7) is sp^2 hybridized, C(8) is sp^3. There are significant changes in the M_2C_2 four-membered ring which cannot however be accounted for solely on the basis of hybridization differences at C_α and C_β. Closer examination of distances C, D, B, and E in Figure 4 reveals the following: (i) As C=N double-bond character increases down the triad, the C_α–C_β distance B increases to a value in **3c** (1.496 (13) Å) close to what would be expected for a normal $C(sp^2)$–$C(sp^3)$ single bond (~1.51 Å). (ii) The metal–carbon distances D and E are distinctly different, with the

(22) If the average unbridged M–M bond lengths in $M_3(CO)_{12}$, M = Fe, Ru, Os, are taken as the normal M–M single-bond distances in group 8 complexes, the values would be (a) 2.673 Å, M = Fe (Wei, C. H.; Dahl, L. F. *J. Am. Chem. Soc.* **1969**, *91*, 1351); (b) 2.8542 Å, M = Ru (Churchill, M. R.; Hollander, F. J.; Hutchinson, j. P. *Inorg. Chem.* **1977**, *16*, 2655); (c) 2.877 Å, M = Os (Churchill, M. R.; DeBoer, B. G. *Inorg. Chem.* **1977**, *16*, 878).

(23) (a) Hoffman, D. M.; Hoffmann, R. *Inorg. Chem.* **1981**, *20*, 3543. (b) Shaik, S.; Hoffmann, R.; Fisel, C. R.; Summerville, R. H. *J. Am. Chem. Soc.* **1980**, *102*, 4555. (c) Summerville, R. H.; Hoffmann, R. *J. Am. Chem. Soc.* **1979**, *101*, 3821.

(24) Merenyi, R. *Adv. Org. Chem.* **1976**, *9*, 90; Imminium Salts in Organic Chemistry, Part 1.

(25) *Molecular Structures and Dimensions*; Kennard, O., Watson, D. G., Allen, F. H., Isaacs, N. W., Motherwell, W. D. S., Petterson, R. C., Town, W. G., Eds.; N.V.A. Oosthoek: Utrecht, 1969; Vol. A1, p 52.

(26) Least Squares Plane: 0.6576*x* – 0.2930*y* + 0.6940*z* – 3.5657 = 0. Deviations from this plane are Ru(1)–0.015 Å; N–0.024 Å; C(7) +0.058 Å; C8 –0.019 Å.

differences in hybridization at C(7) and C(8) accounting for less than one-third of the discrepancy. A plausible explanation of these facts is that there is some multiple-bond character in the M(1)–C(7) bond, i.e., C(7) has carbenoid character. There are relatively few other binuclear group 8 complexes with which to compare **3a–c**. There is however a formal similarity to the ketenyl complex $[(\eta^5\text{-}C_5H_5)_2Ru_2(CO)_2\{\mu\text{-}C(O)CH_2\}]$[27] in which a four-membered ring M–C–C–M is also present. It is interesting that while the Ru–Ru bond length in the latter (2.814 (1) Å) is longer than in **3b** (2.7896 (4) Å), the C(sp^3) – C(sp^2) bond length in the bridge 1.450 (5) Å is actually shorter (cf. **3b** 1.468 (5) Å). The Ru–C bond length to the ketenyl carbonyl (2.105 (3) Å) is very similar to that in **3b** (2.110 (4) Å). In *mononuclear* carbene complexes of ruthenium $Ru\text{–}C_{carb}$ distances lie in the range 1.90–2.13 Å[28] with the distance D in **3b** lying at the top end of this range.

Several examples of binuclear molecules are known in which the C_2 unit has double-bond character. Thus the diosmacyclobutene $Os_2(CO)_8(\mu\text{-}\eta^1\text{:}\eta^1\text{-}MeO_2CC{=}CCO_2Me)$[29] has a C=C bond distance of 1.33 (1) Å, markedly shorter than in **3c** and consistent with a full olefinic linkage. The triethyl phosphite adduct of **1a**, namely, $Fe_2(CO)_6[\mu\text{-}C\{P(OEt)_3\}CPh](\mu\text{-}PPh_2)$,[7b] also has a four-membered Fe_2C_2 ring system, but again the C–C distance (1.34 (2) Å) is far shorter than in **3a**.

The formulation of **3a–c** as complexes of bridging 2-amino-1-metallacarbenes prompted a search for related binuclear and cluster bound ligands. Although the first examples of $\eta^1\text{:}\eta^2$-ethylidene ligands of this type were synthesized several years ago as the products of nucleophilic attack by amines on $\mu_2\text{-}\eta^2$-acetylides, recent work has revealed that bridging electron-rich carbenes analogous to those in **3a–c** may be generated via direct reaction of electron-rich acetylenes with metal carbonyls[30] or via dehydrogenation and isomerization of μ_2-CHCH=NEt_2 ligands on a trinuclear osmium framework.[31] Notable examples of molecules for which X-ray crystallography has demonstrated the presence of bridging 1-metalla-2-aminocarbene ligands are $Fe_2(CO)_7\{C_2(CH_3)N(C_2H_5)_2\}$[30] and $Os_3(CO)_9\{\mu_3\text{-}CHCN(C_2H_5)_2\}(\mu\text{-}H)_2$.[31] Addition of O–H or N–H groups across $\mu_3\text{-}\eta^2$-acetylides also affords hydrocarbyl groups which likely have similar structural features.[4a] In all of these molecules the carbenic character of the coordinated carbon atom is enhanced by electron donation from an electron-releasing NR_2 or OR substituent.

Chart I

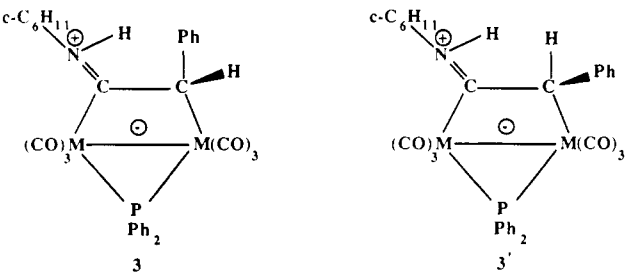

Whether binuclear and cluster complexes of intact electron-rich acetylenes in general have structures more closely resembling those of $Fe_2(CO)_7\{C_2(CH_3)N(C_2H_5)_2\}$[30] or $Os_3(CO)_9\{\mu_3\text{-}CHCN(C_2H_5)_2\}(\mu\text{-}H)_2$[31] than typical $\mu_3\text{-}\eta^2\text{-}\parallel$ or $\mu_3\text{-}\eta^2\text{-}\perp$ bonding modes is a question that may have relevance to the broader problem of alkyne scission reactions on clusters.[32]

The carbon atom C(8) is a chiral center, but since the crystal is centrosymmetric, there is a 1:1 ratio of molecules related by an inversion center, and both absolute configurations of C(8) are present in the solid. In principle amine addition across the acetylide triple bond could result in two possible isomers, the one observed in the X-ray structure with the proton on C(8) facing the phosphido bridge or with the phenyl group of the original acetylide oriented toward the μ-PPh_2 group (Chart I). There is no spectroscopic evidence for isomer interconversion. Thus the addition across the acetylide is stereospecific. Presumably steric interactions between the phenyl group on C(8) and the phosphido bridge phenyl groups disfavors the second isomeric conformation.

With an increase in M–M distance in **3a–c** compared to the precursors **1a–c**, the M–P–M angle opens by almost a full degree (71.70–72.45 (5)° **1a–3a**; 72.03 (1)–73.00 (2)° **1b–3b**; 72.61 (7)–73.52 (6)° **1c–3c**), but the M–P distances remain relatively constant. The values for M–P–M are within the normal ranges for μ-PPh_2 groups across strong group 8 M–M bonds.[18]

Acknowledgment. We are grateful to NSERC for financial support of this work in the form of grants (to A.J.C.) and scholarships (to A.A.C. and L.H.R.).

Supplementary Material Available: Tables of anisotropic thermal parameters and phenyl ring bond lengths and bond angles for **3b** and **3c** (4 pages); tables of structure factors for **3b** and **3c** (41 pages). Ordering information is given on any current masthead page.

(27) Doherty, N. M.; Fildes, M. J.; Forrow, N. J.; Knox, S. A. R.; Macpherson, K. A.; Orpen, G. A. *J. Chem. Soc., Chem. Commun.* **1986**, 1355.
(28) Gallop, M. A.; Roper, W. R. *Adv. Organomet. Chem.* **1986**, *25*, 121.
(29) Burke, M. R.; Takats, J. *J. Organomet. Chem.* **1986**, *302*, C25.
(30) Cabrera, E.; Daran, J. J.; Jeannin, Y.; Kristiansson, O. *J. Organomet. Chem.* **1986**, *310*, 367.
(31) Adams, R. D.; Tanner, J. T. *Organometallics* **1988**, *7*, 2241.
(32) See, for example: (a) King, R. B.; Harmon, C. A. *Inorg. Chem.* **1976**, *15*, 879. (b) Fritch, J. R.; Vollhardt, K. P. C. *Angew. Chem., Int. Ed. Engl.* **1980**, *19*, 559. (c) Chi, Y.; Shapley, J. R. *Organometallics* **1985**, *4*, 1901. (d) Hriljac, J. A.; Shriver, D. F. *J. Am. Chem. Soc.* **1987**, *109*, 6010. (e) Nuel, D.; Dahan, F.; Mathieu, R. *Organometallics* **1985**, *4*, 1436.